1. Basic Concepts

1.1 ELECTROMAGNETIC WAVES

The radiation field from a transmitting antenna is characterized by the complex Poynting vector E x H* in which E is the electric field and H is the magnetic field. Close to the antenna the Poynting vector is imaginary (reactive) and (E,H) decay more rapidly than 1/r, while further away it is real (radiating) and (E,H) decay as 1/r . These two types of fields dominate in different regions in space around the antenna. Based on this characterization of the Poynting vector, we can identify three major regions (Figure 1).
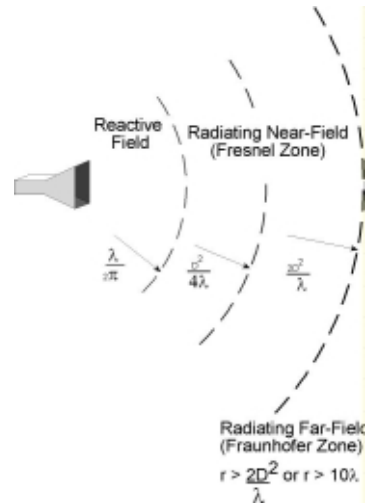

Figure 1: Radiating Regions

1.1.1. Reactive Field

This region is the space immediately surrounding the antenna. The extent of this region is $0 < r < \lambda/2\pi$, where l is the wavelength. In this space the Poynting vector is predominantly reactive (non-radiating), has all three components in spherical coordinates (r,θ,ϕ) and decays more rapidly than 1/r.

1.1.2 Radiating Near-Field

Beyond the immediate neighborhood of the reactive field the radiating field begins to dominate. The extent of this region is $\lambda/2\pi < r < 2D^2/\lambda$, where D is the largest dimension of the antenna. This region can be divided into two subregions. For $\lambda/2\pi < r < D^2/4\lambda$ the fields decay more rapidly than 1/r and the radiation pattern (relative angular distribution of the field) is dependent on r. For $D^2/4\lambda < r < 2D^2/\lambda$ the fields decay as 1/r, but the radiation pattern is dependent on r. The radiation pattern is equal to the Fourier transform of the aperture distribution with a phase error of more than 22.5°. The phase error is dependent on r (for $r \rightarrow \infty$ the phase error is equal to zero). This region is often referred to as the Fresnel zone, a terminology borrowed from optics.

1.1.3 Radiating Far-Field

Beyond the radiating Near-Field region r > $2D^2/\lambda$ or r > 10l (criterion for small antennas) the Poynting vector is real (only radiating fields) and has only two components in spherical coordinates (θ,ϕ). The fields decay as 1/r and the radiation pattern is independent of r. The radiation pattern in this region is approximated by the Fourier transform of the aperture distribution with a phase error of less than 22.5°. This region is often referred as the Fraunhofer zone, a terminology borrowed from optics.

1.2 ANTENNA PARAMETERS

1.2.1 Antenna

The antenna is a device which transforms guided electromagnetic signals into electromagnetic waves propagating in free space. It can be used for reception and transmission.

1.2.2 Polarization

Polarization is the property of the electric field vector that defines variation in direction and magnitude with time. If we observe the field in a plane perpendicular to the direction of propagation at a fixed location in space, the end point of the arrow representing the instantaneous electric field magnitude traces a curve. In the general case, this curve is an ellipse (Figure 2). The ellipse can be characterized by the axial ratio (AR), the ratio of the two major axes and its tilt angle t. Polarization may be classified as linear, circular or elliptical according to the shape of the curve. Linear and circular polarization are special cases of elliptical polarization, when the ellipse becomes a straight line or circle, respectively. Clockwise rotation of the electric field vector is designated as right-hand polarization (RH) and counterclockwise rotation is left-hand polarization (LH), for an observer looking in the direction of propagation.
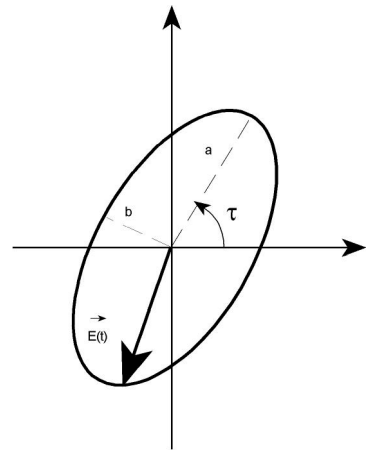

Figure 2: Elliptical Polarization

1.2.3 Input Impedance and VSWR

Input impedance is defined as the impedance presented by the antenna at its terminals or the ratio of the voltage to current at its terminals. If the antenna is not matched to the interconnecting transmission line, a standing wave is induced along the transmission line. The ratio of the maximum voltage to the minimum voltage along the line is called the Voltage Standing Wave Ratio (VSWR).

1.2.4 Directivity

The directivity is a measure that describes the directional transmitting properties of the antenna. It is defined as the ratio of the antenna radiation intensity in a specific direction in space over the radiation intensity of an isotropic source for the same radiated power. There are cases in which the term directivity is implied to refer to its maximum value.

1.2.5 Gain

The gain of the antenna is closely related to the directivity, but takes into consideration the losses in the antenna as well as its directional capabilities.

1.2.6 Efficiency

The antenna efficiency is the ratio of directivity to gain. It takes into consideration all the power lost before radiation. The losses may be due to mismatch at the input terminals, conduction losses, dielectric losses and spillover losses.

1.2.7 Effective Isotropically Radiated Power (EIRP)

The Effective Isotropically Radiated Power (EIRP) is a figure of merit for the net radiated power in a given direction. It is equal to the product of the net power accepted by the antenna and the antenna gain.

1.2.8 Radiation Pattern

The antenna radiation pattern is the display of the radiation properties of the antenna as a function of the spherical coordinates (θ,ϕ). In most cases, the radiation pattern is determined in the Far-Field region for constant radial distance and frequency. A typical radiation pattern is characterized by a main beam with 3 dB beamwidth and sidelobes at different levels (Figure 3). The antenna performance is often described in terms of its principal E- and H-plane patterns. For a linearly polarized antenna, the E- and H-planes are defined as the planes containing the direction of maximum radiation and the electric and magnetic field vectors, respectively.
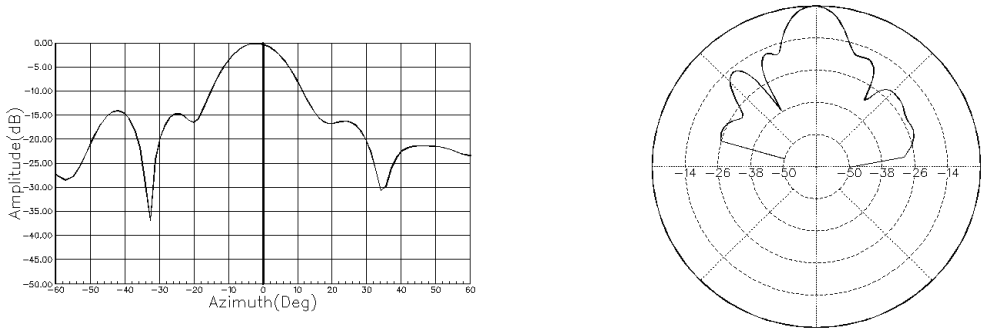

Figure 3: Radiation patterns
(a) Rectangular Form   (b) Polar Form

1.2.9 Antenna Noise Temperature

The antenna noise temperature is a measure that describes the noise power received by the antenna at a given frequency. It can be obtained by integrating the product of the antenna directivity and the brightness temperature distribution of the environment over the entire space. The brightness temperature of the environment is dependent on many noise sources: cosmic, atmospheric, man-made and ground. The noise power received at the antenna terminals is equal to KTaB in which K is Boltzman coefficient, Ta is the antenna noise temperature and B is the bandwidth of the system receiver.

1.2.10 G/T Parameter

A convenient figure of merit proportional to the signal-to-noise ratio received by the antenna is the value of G/T, in which G is the antenna gain and T is the receiving system noise temperature in degrees Kelvin. T is the summation of the antenna noise temperature and the   RF chain noise temperature from the antenna terminals to the receiver output.

1.3 RELATED TERMS

1.3.1 Mixers

The mixer is a critical component in the instrumentation of antenna measurements. It converts RF power at one frequency into power at another frequency to make signal processing easier and less expensive. It is a nonlinear device, which mixes the input RF signal at a frequency, f_{RF}, with a local oscillator signal at frequency, f_{LO}, to obtain a signal at an intermediate frequency f_{IF}. The relationship among the frequencies is $f_{IF} = f_{RF} \pm nf_{LO}$, where n is the harmonic mixing number. At the IF port a filter is connected to reject all spurious signals except the f_{IF} frequency. If the mixer uses only the basic frequency of the local oscillator (n = 1) it is called fundamental, while if it uses higher harmonics to obtain the IF frequency it is called a **harmonic** mixer. Harmonic mixing is a cost-effective technique used in the microwave frequency range to operate over an extremely wide bandwidth with a single local oscillator that is tunable only a portion of the required frequency band. The mixing efficiency is called the conversion loss and is defined as the ratio of the IF output power to the RF input power. The typical conversion loss of a broadband harmonic mixer employing the fundamental LO frequency is between 6 and 9 dB. As the harmonic number employed increases the mixer conversion loss increases by approximately 6dB for each doubling of the harmonic mixing number. Consequently, the system sensitivity is reduced with the increase in the operating frequency. In antenna measurement systems, a harmonic mixer with only two ports is common. One port is used for the RF input, while the other is common to the local oscillator and the IF signals. This configuration is advantageous, since a single coaxial cable can connect the remote Antenna Under Test (AUT) to the receiver.

2. Antenna Measurements

The testing and evaluation of the antenna parameters is performed in antenna ranges. Typically, there exist indoor and outdoor ranges with associated limitations for both. Outdoor ranges are not protected from environmental conditions, while indoor ranges are limited by space restrictions. Indoor ranges make use of anechoic chambers, which are chambers lined with radar absorbing material to eliminate reflections from the walls. There are two basic forms of chambers:
rectangular anechoic chambers and tapered anechoic chambers.   Rectangular chambers are typically used for frequencies above 1 GHz, while for frequencies below 1 GHz tapered chambers are used.

Various methods exist to measure the antenna parameters: radiation pattern directivity, gain and polarization. Some of the methods require the Far-Field criterion and uniform plane illumination and some can be performed in the Near-Field of the Antenna Under Test (AUT).

2.1 RADIATION PATTERN MEASUREMENT

The patterns of antennas can be measured in transmit or receive mode. Some types of antennas must be measured under both transmit and receive conditions. In general, the pattern of an antenna is three-dimensional (Figure 5). Because it is not practical to measure a three-dimensional pattern, a number of two-dimensional patterns are measured. A two-dimensional pattern is referred to as a pattern cut. Pattern cuts can be obtained by fixing f and varying q (elevation pattern), or fixing q and varying f (azimuth pattern). To achieve the desired pattern cuts, the mounting structure of the system must have the capability to rotate in various planes. This can be accomplished by using different types of positioners such as Elevation-over-Azimuth (EL/AZ) or Azimuth-over-Elevation (AZ/EL) mounts.
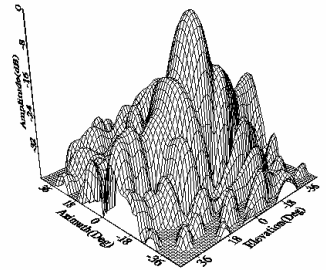

Figure 5: Three-Dimensional Radiation Pattern

2.2 DIRECTIVITY MEASUREMENT

The directivity can be computed by using measurements of the radiation pattern. By definition, the directivity is equal to the ratio of 4þ times the maximum radiation intensity to the total radiated power by the antenna. The radiated power is evaluated numerically by integrating the radiation intensity over the entire space.

2.3 GAIN MEASUREMENT

There are two basic methods that can be used to measure the gain of an antenna: absolute gain and gain comparison techniques. The absolute gain method requires no a priori knowledge of the transmitting or receiving antenna gain. If the receiving and transmitting antennas are identical, one measurement and use of the transmission formula is sufficient to determine the gain. If the antennas are different, three antennas and three measurements are required to formulate a set of three equations with three unknowns to determine the gain of the AUT. In the gain comparison method, precalibrated Standard Gain Antennas are used to determine the absolute gain of the AUT.

2.4 POLARIZATION MEASUREMENT

The polarization measurement method requires that a linearly polarized antenna, usually a dipole or a small horn, is rotated in the plane of polarization, which is taken to be normal to the direction of the incident field, and the output voltage of the probe is recorded. The recorded signal describes a polarization pattern for an elliptically polarized antenna. The polarization ellipse is tangent to the polarization pattern, and can be used to determine the axial ratio and the tilt angle of the AUT.

3. Far-Field Measurements

3.1 FAR-FIELD RANGES

The Far-Field measurements can be performed in outdoor or indoor ranges. In general, there are two basic types of Far-Field antenna ranges: reflection and free space ranges. In the reflection range, we create in the region of the AUT, a constructive interference between the direct rays from the transmitting antenna and the specular reflection from the ground. In the free space ranges the reflections from the ground are minimized. There are three types of free space ranges: elevated ranges, slant ranges and compact ranges.

3.1.1 Elevated Range (Free Space)

Elevated ranges are usually designed to operate mostly over smooth terrain. The antennas are mounted on towers or on roofs of adjacent buildings (Figure 6). The range length r is designed to meet the Far-Field criterion r > 2D2/λ, in which D is the largest dimension of the source or AUT. The height of the AUT, h_r, is determined by two criteria related to the source antenna. The source antenna should be chosen so that the amplitude taper over the AUT is typically no greater than 0.25 dB, to ensure uniform illumination. In addition, to minimize the range reflections, its first null points toward the base of the test tower, ensuring that the range surface intercepts only sidelobe energy. These two criteria determine the height of the AUT to be h_r > 4D. In elevated ranges diffraction fences are sometimes used to further minimize the reflections from the ground. There are two cautions that should be emphasized. First, the diffraction fence should not intercept the main beam of the source antenna. Second, the top edge of the fence should not be straight knife edge, but rather serrated to reduce the edge diffraction.
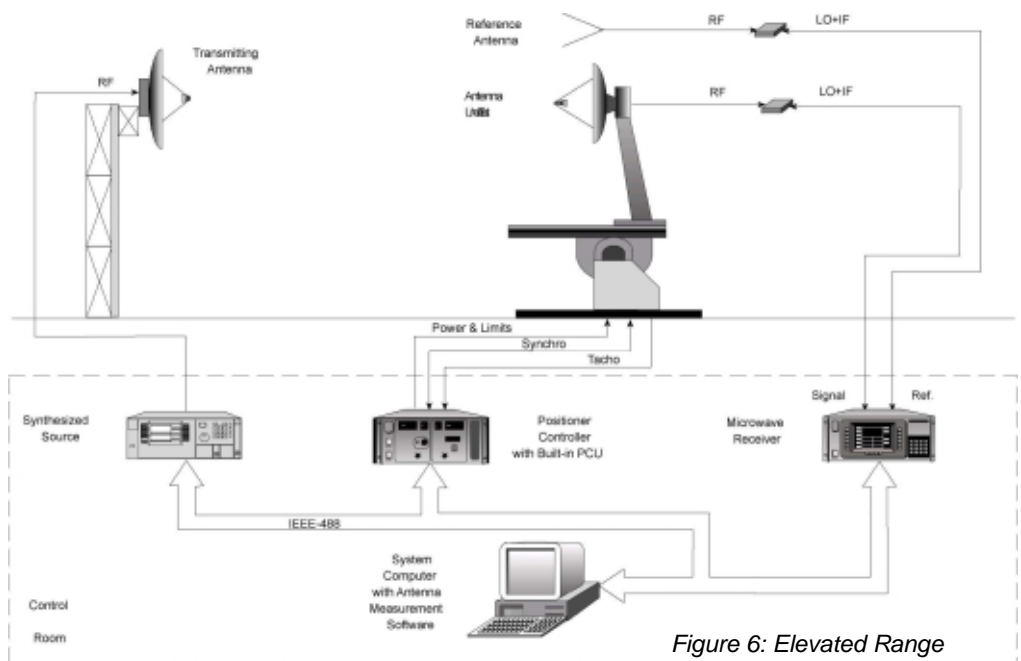

Figure 6: Elevated Range

3.1.2 Ground Reflection Range

In the ground reflection range, the specular reflection from the ground is used to obtain a uniform phase and amplitude distribution over the AUT (Figure 7). Accordingly, it is essential that the range surface be smooth. The range length r is designed to meet the Far-Field criterion $r > 2D^2/\lambda$, in which D is the largest dimension of the source or AUT. The heights of the source and AUT are chosen so that the AUT is centered on the first interference lobe of the direct and specular reflected rays. This criterion determines the relation between the source height, h_t , and the AUT height, h_r, to be $h_t » \lambda/4h_r$. If the amplitude taper over the AUT is required to be no more than 0.25 dB, the height of the AUT should meet the criterion $h_r > 3.3D$.
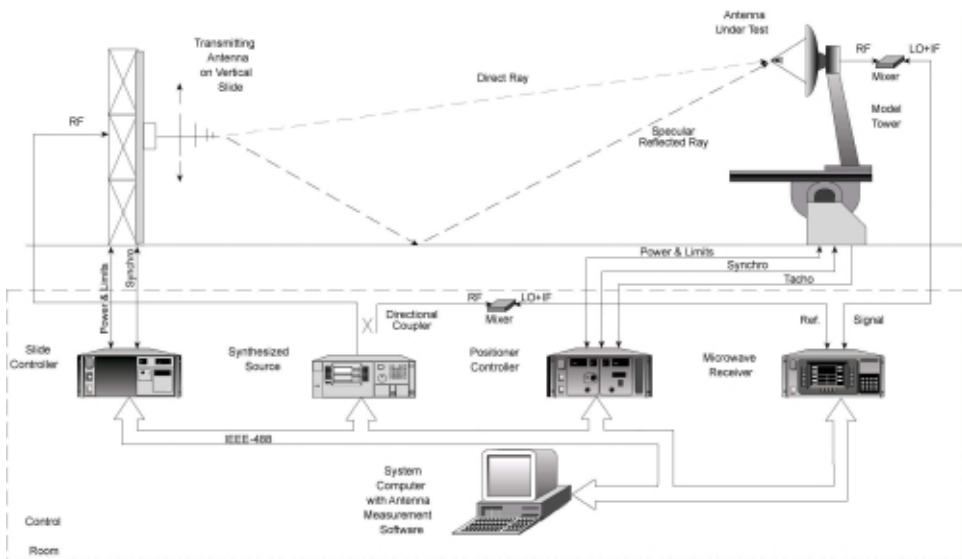

Figure 7: Full Reflection Range

3.1.3 Slant Range

A slant range is one in which the source antenna is located close to the ground and the AUT is mounted on a tower (Figure 8). The source antenna points toward the center of the AUT and its first null points toward the tower base. It is desirable that the tower of the AUT be constructed of nonconducting materials to reduce reflections. Slant ranges, in general, require less real estate than elevated ranges.
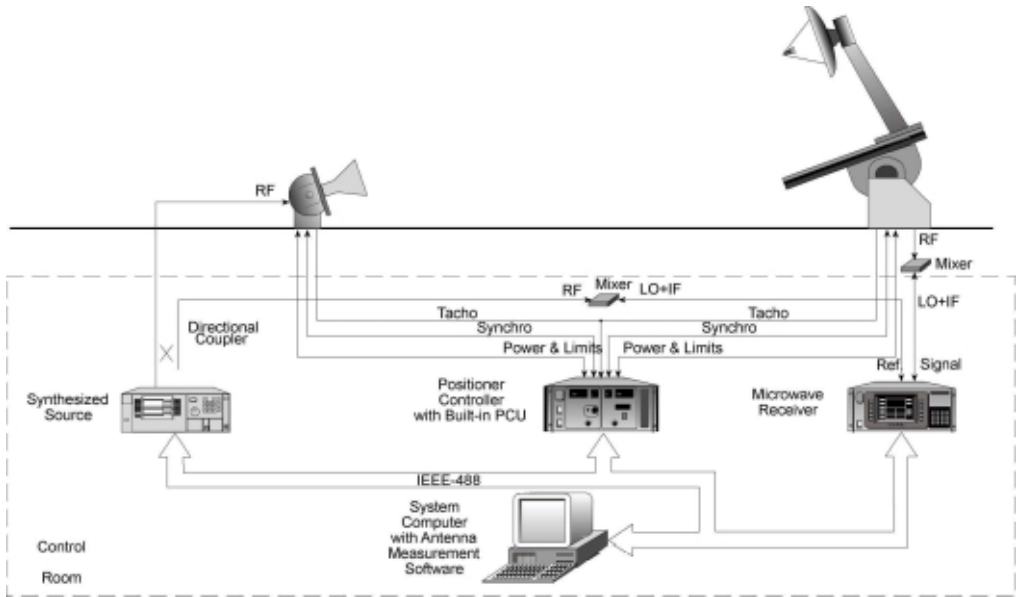

Figure 8: Slant Range

3.1.4 Compact Range

Antenna measurements require that the AUT be illuminated by a uniform plane wave. This requirement is achieved in the far field for range length r > 2D2/λ, which in many cases dictates large distances. A compact range creates a plane wave field at distances considerably shorter than those needed under conventional Far-Field criteria. The required compact range is usually so short that the implementation can be accomplished indoors. In the compact range, a uniform plane wave is generated by a large parabolic reflector (Figure 9).
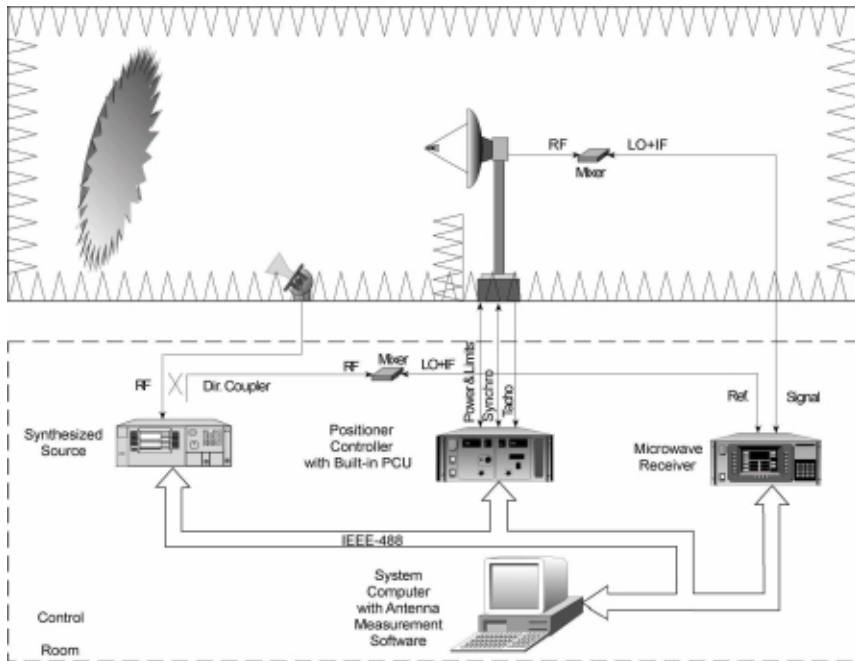

Figure 9: Compact Range

The parabolic reflector provides the means to convert a spherical phase front from the feed into a planar phase front close to its aperture. The AUT may be located near the aperture of the reflector in order to illuminated by a uniform plane wave.

There are a number of factors which affect the compact range performance: aperture blockage, surface accuracy, edge diffraction, depolarization effects, direct coupling between the feed and AUT and room reflections.

The aperture blockage is reduced by using an offset reflector system. In the design of the main reflector the surface accuracy is chosen to be very stringent to reduce the amplitude and phase variation of the reflected plane wave. The edge diffraction is reduced by using serrated or blended (e.g. rolled) edges. The depolarization effects are minimized by using an offset Cassegrain system or increasing the reflector focal length. Direct coupling between the feed and AUT is reduced by a proper choice of geometry and shielding. The room reflections are minimized by using absorbing materials on the walls.

3.2 ERRORS IN FAR-FIELD MEASUREMENTS

The signal received by the tested antenna is composed of the direct signal, E_d, from the source and the reflected signal, E_r, from specular ground reflection and surrounding objects present in the range. In elevated ranges this reflected signal is the major cause for error in radiation pattern and gain measurements. Figures 10a and 10b show the dependence of the error on the ratio Er / Ed for in-phase and out- of-phase reflected signals. For decibel ratios E_r / E_d of less than -25 dB the error for in-phase and out-of-phase reflected signals is symmetrical. Figure 11 shows the peak-to-peak error (in-phase and out-of-phase reflections) in the sidelobe level due to the range reflections, with the range reflectivity being the parameter.
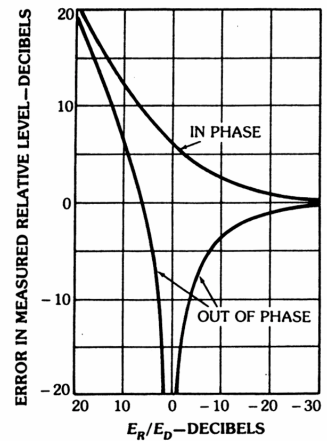
(a)
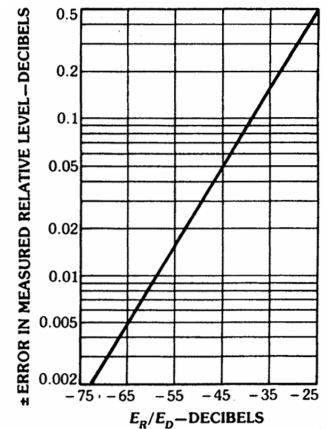
(b)

Figure 10: Error Limits in Measured Pattern Coherent Levels Due to Extranous Signals. (After ANSI/ IEEE)
(a) Signal Ratios of +20 to –30 dB
(b) Below –25 dB

The system is calibrated to exclude all the frequency-dependent components except the reflections from the ground, and the received signal versus frequency is recorded. The reflection level of the range is determined from the ratio of the maximum and minimum received power. The same effect can be obtained at a fixed frequency by raising the source antenna and recording the received signal, while the AUT is stationary. The third method employs time domain techniques and range gating, which help to separate the direct signal from the reflected signal and display only the direct signal. This is the most accurate method to eliminate the range reflections.

An additional type of error in far-field ranges is caused by the finiteness of the antenna range length, r. The exact radiation pattern is defined for $r \to \infty$, while in a practical range the length is finite. The finiteness of the range introduces a phase error on the antenna's aperture, which perturbs the measured radiation pattern. Figure 12 shows typical radiation patterns for a 30 dB Taylor aperture distribution measured on different range lengths $r = nD^2/\lambda$, where n=1,2,... and D is the aperture diameter. One can observe that small ranges cause null filling and an increase in the sidelobe level.

The range surface irregularity affects the ground reflections and causes phase and amplitude variations along the tested antenna aperture. The ripple can be measured by probing the field at the receiving end on the tested antenna aperture, and it can be minimized by taking special care of range smoothness. This type of error is especially important in a full reflection range.

In outdoor ranges external signals may interfere with the direct signal and cause measurement errors. Their effect can be eliminated by using sharp filters.
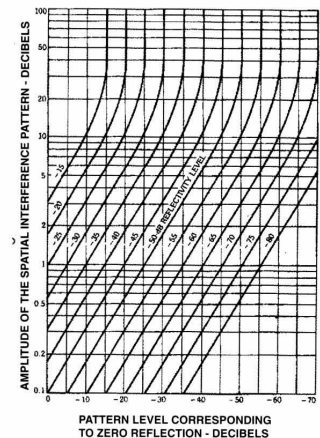

Figure 11: Amplitude of spatial interference pattern for a given reflectivity level
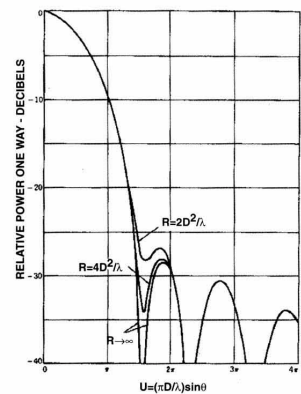

Figure 12: Calculated radiation patterns illustrating the effect of quadratic phase errors encountered in measuring patterns at the ranges indicated.

3.3 SITE CONSIDERATTIONS

Four types of Far-Field ranges have been presented. The most accurate antenna range is the indoors compact range, since all its errors can be controlled and minimized. Its size is also minimal compared to the other ranges. It is limited by the maximum AUT size (the chamber's physical dimensions) and the lowest usable frequency range (absorbing material size and reflector edge treatment). These limitations have a cost impact. The size of the other three ranges is determined by the far-field criterion r > 2D2/l. The ground reflection range uses the surface reflections to obtain uniform field distribution along the AUT aperture. However, this fact imposes very strict requirements on the range smoothness (related to the highest usable frequency), which has cost and maintenance impact. The measurement errors due to ground reflections in the slant range are lower than in a comparable elevated range; however, its receiving tower is higher than in the elevated range. This fact puts a limit on the maximum antenna size to be lifted at the top of the tower. The elevated range is common in microwave measurements for medium-size antennas. The ground reflection errors encountered in this type of range are minimized by using diffraction fences, or by using measurement techniques to determine precisely the reflection level and subtract it from the measurement.
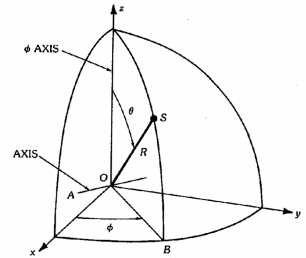

Figure 13: The two orthogonal rotation axes required for a spherical-coordinate

3.4 POSITIONER SELECTION CRITERIA

A practical way to obtain the radiation pattern is to record the signal received by the AUT through its motion in spherical coordinates (θ, ϕ), while keeping the probe antenna stationary. Two orthogonal rotational axes are required in order to provide the relative motion of the AUT with respect to the source antenna. Figure 13 illustrates these axes, O_A (θ rotational axis) and OZ (f rotational axis). The AUT is located at the origin, while the source antenna is located at point S, with OS being the line of sight between them. Note that both OS and OZ are always perpendicular to OA. Moreover, to minimize radiation pattern measurement errors, the phase center of the antenna should coincide with the axes-crossing point of the positioner.
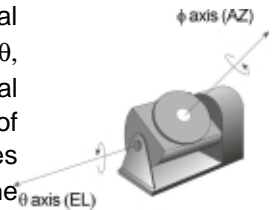

Figure 14: The three basic

There are various positioners that provide the θ and ϕ rotations. Figure 14 shows the most common types of positioners and their coordinate systems: (a) azimuth-over-elevation (AZ/EL), (b)

Antenna Measurement Theory

elevation-over- azimuth (EL/AZ) and (c) azimuth-over-elevation-over-azimuth (AZ/ EL/AZ). In the AZ/EL positioner, the azimuth positioner provides 360° motion around the ϕ axis, while the elevation positioner provides a limited motion around the θ axis. In the EL/AZ positioner, the elevation positioner provides the motion around the θ axis, while the azimuth positioner provides the motion around the Φ axis. The AZ/EL/AZ positioner is similar to the AZ/EL positioner, but has an extra F axis for the purpose of alignment with the source antenna. The axes-crossing point of all these positioners is lower than the phase center of the AUT, therefore measurement errors may be introduced. On the AZ/EL positioner, the AUT phase center is relatively closer to the axes-crossing point compared to the EL/AZ positioner, but its alignment to the source (without affecting the accuracy of the measured radiation patterns) is limited. The AZ/EL/AZ combines the advantages of both AZ/EL and EL/AZ positioners and can also be used as a polarization positioner. Polarization measurements can be performed if the source antenna (linear polarization) is assembled on a special positioner and rotated at high speed.
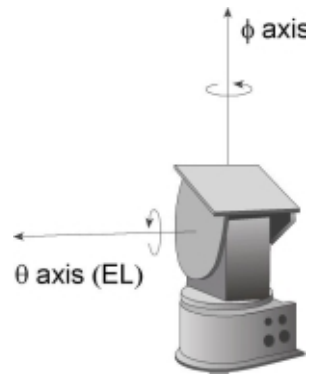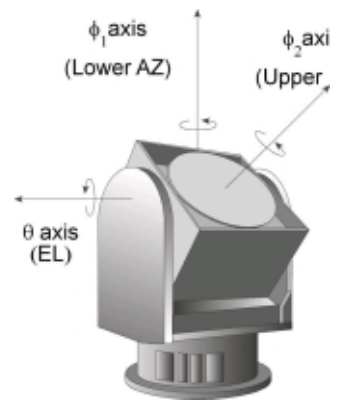

Figure 14 (b) Elevation-over-azimuth positioner

Figure 14 (c) Roll-over-azimuth positioner

4. Near-Field Measurements

The dimensions of a conventional test range can be reduced by making measurements in the Near-Field of the AUT, and then using analytical methods to transform the measured Near-Field data to compute the Far-Field radiation characteristics. Such techniques are usually used to measure patterns and gain.

4.1 TYPES OF NEAR-FIELD SETUPS

The Near-Field measured data (amplitude and phase distribution) is acquired by using a probe to scan the field over a preselected geometrical surface, which may be a plane, a cylinder, or a sphere. The measured data is then transformed to the Far-Field using analytical methods. The complexity of the analytical transformations increases from the planar to the cylindrical, and then to the spherical surfaces.

4.1.1 Planar

In the planar scanning technique, a probe antenna is moved in a plane situated in front of the AUT and the received signal (amplitude and phase) is recorded. The position of the probe is characterized by the coordinates (x,y,z_0) in the xyz coordinate system of the AUT. During the scanning, z_0, is kept constant, while x and y are varied. The distance z_0 is approximately 3λ - 10λ to avoid sampling of the reactive energy of the AUT. The dimensions of the Near-Field scanning aperture must be large enough to accept all significant energy from the AUT. The

Figure 15: Maximum scan size

scan dimensions, D_s, have to meet the criterion $D_s > D+2z_0\tan\theta$, where D is the largest AUT dimension and θ is the maximum processed radiation pattern angle (Figure 15). For a specific scanner with an allowable scan area D_p, this criterion determines the maximum and minimum AUT size ($D_{min} \approx 2\lambda$).
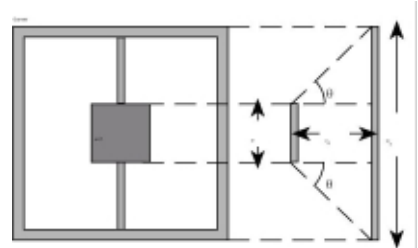
Antenna Measurement Theory

The measured Near-Field data E (x,y,z_0) is transformed into the plane wave spectrum E (k_x,k_y) in the K-space, by a two-dimensional Fourier transform. The coordinates (k_x,k_y) in the K-space are related to the spherical coordinates (θ,ϕ), through the relationships $k_x=k\sin\theta\cos\phi$, $k_y= k\sin q\sin f$ and $k=2\pi/\lambda$. The antenna plane wave spectrum is distorted by the angular response of the probe. This effect can be deconvoluted from the AUT angular response by taking the ratio of the total plane wave spectrum to the probe spectrum. This operation is known as probe correction. The plane wave spectrum in the visible range, $-k < k_x,k_y < k$, is proportional to the radiation pattern $F(\theta,\phi)$. Accordingly, the radiation pattern can be considered as a spatially band-limited function in the K-space on which Nyquist sampling theory applies and the sampling space can be chosen as $Đ_x=Đ_y=\lambda/2$. This sampling criterion ensures that no aliasing occurs in the visible range. For high-gain antennas we are interested only in a limited angular sector around the AUT main beam.

In these cases, we can increase the sampling space beyond $\lambda/2$ and allow aliasing in the visible range, without affecting the accuracy of the AUT radiation pattern in the main beam and surrounding sidelobes. The increase in the sampling spacing also allows utilizing higher gain probes in the measurement without affecting the accuracy. Three basic types of scans exist in planar Near-Field measurements: rectangular, plane-polar and bi-polar. In the plane-rectangular scan the data is collected on a rectangular grid and processed by the conventional FFT algorithm (Figure 16).
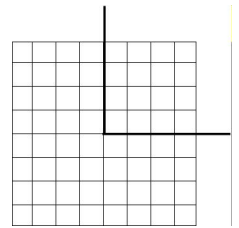

Figure 16: Rectangular scan

In the plane-polar technique, the AUT is rotated around its axis and the probe is attached to a linear positioner placed above the AUT (Figure 17). The combination of the antenna rotation and linear probe motion yields planar Near-Field data collected on concentric rings with data points lying on radial lines. The polar Near-Field data is processed to the far field by a Jacobi-Bessel transform or by interpolation to obtain a rectangular grid for FFT algorithm.
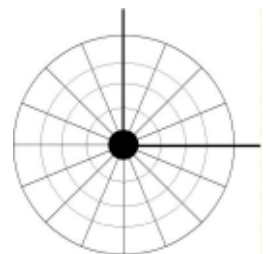

Figure 17: Plane-polar scan

The bi-polar technique is similar to the plane-polar configuration in the sense that the AUT is rotated, but differs in the probe motion. The probe is rotated about a second axis and describes an arc that passes through the AUT axis (Figure 18). The combination of antenna rotation and probe arm rotation yields planar Near-Field data collected on concentric rings with data points lying on radial arcs. The Near-Field data is interpolated into a plane-rectangular grid. The rectangular data is then processed using the FFT to obtain the radiation pattern.
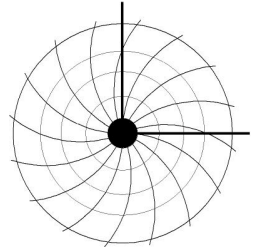
Figure 18: Bi-polar scan

4.1.2 Cylindrical

In the cylindrical scanning technique, the AUT is rotated around the z axis of an xyz-coordinate system in $\Delta\phi$ steps, while the probe is moved on the cylindrical surface at various heights relative to the xy plane in Δz steps (Figure 19). The probe is located at a distance a, which is the smallest cylinder radius enclosing the AUT. The cylindrical scanning enables obtaining the exact azimuth pattern but limited elevation pattern due to the truncation of the scanning aperture in z direction. In accordance with the sampling theory the sampling spacing is determined from $\Delta\phi = \lambda/2a$ and $\Delta z = \lambda/2$. A two-dimensional Fourier transform of the Near-Field data gives the cylindrical vector wave functions that determine the test radiation pattern. The probe response is deconvoluted from the AUT angular response in a similar way as in planar scanning.
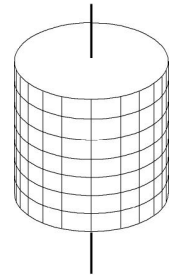
Figure 19: Cylindrical scan

4.1.3 Spherical

In the spherical scanning technique the AUT is rotated around the z axis in $\Delta\phi$ steps and the probe is moved on a circular track in $\Delta\theta$ steps (Figure 20). The radius of the rotation is "a" and is the smallest radius enclosing the AUT. The alternative is to keep the probe stationary and move the AUT in $\Delta\phi$ and $\Delta\theta$ steps. The advantage of spherical scanning is that it delivers the full extent of the AUT three-dimensional pattern.
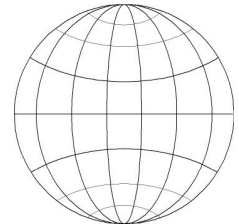
The incident field on the probe is expanded in spherical wave functions. Given the coefficients of these functions, the radiation pattern can be computed. The sampling spacing is determined by the sampling theory to be $\Delta\phi = \Delta\theta = \lambda/2a$.

Figure 20: Spherical scan

4.2 ERRORS IN NEAR-FIELD MEASUREMENTS

The accuracy in Near-Field measurements is determined by four major factors: RF reflections, mechanical errors, truncation errors and system errors.

4.2.1 RF Reflections

In this category we can identify three types of errors: mutual coupling between the probe and the AUT, multipath reflections (walls, scanner and AUT mount), and leakage from the transmitting and receiving systems. The mutual coupling between the probe and the AUT can be minimized by several methods: using absorbing material around the probe, thinning the edge of the probe to minimize the reflective area, using an isolator at the probe data input, and averaging the recorded data of a pair of Near-Field scans separated by $\lambda/4$. The multipath reflections from the walls and the mount can be reduced by using absorbing material on the wall behind the scanner, on the floor, on the scanner and on the mount. Leakage from the transmitting and receiving systems can be minimized by proper shielding and cabling, especially the connectors. This type of error may be discovered by probing a possible signal when the transmitting terminals are terminated.

4.2.2 Mechanical Errors

In this category we include errors due to: imperfect scan surface, misalignment of the scan surface, and probe positioning errors. An imperfect scan surface, which implies deviation from a perfect planar, cylindrical, or spherical surface, may cause random phase errors in the Near-Field data and may affect the accuracy of the computed radiation pattern sidelobe levels. To minimize this type of error, very stringent requirements are set on the scan surface during installation ($\Delta z < \lambda/100$).

If the system collection data repeatability is good, this requirement may be alleviated and correction tables may be used. Misalignment between the scan surface and the phase front of the AUT may cause boresight error of the calculated radiation pattern. To reduce this type of error, stringent calibration techniques with theodolite or lasers are used during installation. Probe positioning errors may cause phase errors in the Near-Field collected data and perturb the sidelobe level of the AUT radiation pattern. This type of error may be minimized by using a set of lasers to measure the exact position of the probe during the scan or by using correction tables prepared during the system calibration stage.

4.2.3 Truncation Error

A truncation of the scan surface in planar and cylindrical scanning results in two effects: gain reduction due to lower integrated power and introduction of spurious sidelobes in the AUT radiation pattern. To minimize this error, several scans with different truncations are measured and the Far-Field is compared. If the measured power level at the edge of the scan surface is significantly lower (> 30 dB) than the level at its center, then the effect of this error is insignificant.

4.2.4 System Errors

This category includes errors related to receiver nonlinearity, source and receiver drift, and phase variation of the cables. Nonlinearity of the receiver may result in the perturbation of the sidelobe level of the AUT radiation pattern. A simple test to verify the linearity is to repeat the measurement at two different attenuation levels and compare the Far-Field patterns. The source and the receiver may encounter amplitude and phase drift during the measurement. The drift can be measured by rescanning at the center of the original scan aperture after the data acquisition sequence is completed. The probe motion may introduce phase errors due to unstable cable phase. This type of error may be reduced by using high quality cables, and it can be verified by repeating the measurement for a different routing of the RF cables.

4.3 SITE CONSIDERATIONS

Three major types of Near-Field ranges have been presented. The choice is primarily determined by the antenna to be measured. The planar system is best suited for high-gain and flat antennas, since the measured field is restricted to a plane. It is also the lowest cost system, since it involves relatively simple hardware and its computational complexity is relatively low. The cylindrical system fits antennas with cylindrical symmetry. It gives the exact radiation pattern in the azimuth plane (360° coverage), but a truncated pattern in elevation. The spherical system is the most accurate system for the entire space and essential for low-gain and omnidirectional antennas. It is also best suited for antennas with controlled sidelobe levels in the entire space. Its deficiency is in its relatively complex computations and the related processing time.

5. Radome Measurements

Radome measurements are performed in order to characterize the electrical parameters of the radome. The most commonly measured parameters are the Radome Boresight error and the Radome Transmission Efficiency.

5.1 RADOME BORESIGHT ERROR (RBE)

When the radome is placed over an antenna that has a boresight null (e.g. monopulse or conical scan antennas), then the Radome Boresight error (RBE) is the shift induced by the radome in the direction of the boresight null. For antennas with a boresight null, the RBS is the angular difference in the direction of the boresight null induced when the radome is placed over the antenna (Figure 21).

For antennas without a boresight null, the RBE is the angular difference in the direction of the main lobe induced when the radome is placed over the

Figure 21: Radome Boresight Shift

antenna. In general, the RBE depends on the relative position between the radome and the antenna. Therefore, it is usually measured as a function of the relative angle between the radome and the antenna.
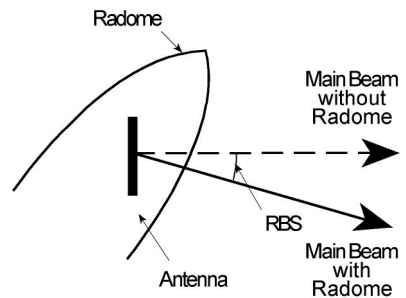
5.2 RADOME BORESIGHT ERROR SLOPE (RBES)

The Radome Boresight Error Slope (RBES) is the rate of change of the RBE across the radome. It can be computed from the RBE results as a function of the relative angle between the radome and the antenna.

5.3 RADOME TRANSMISSION EFFICIENCY AND RADOME TRANSMISSION LOSS

These are two different ways to represent the ratio between the electromagnetic power transmitted through the radome in the direction of the main beam and the electromagnetic power transmitted in the same direction in the free space (in the absence of the radome). The Radome Transmission Efficiency is expressed in percent (%) and the Radome Transmission Loss is expressed in dB, both as a function of the relative angle between the radome and the antenna.

References

ANSI/IEEE Standard Test Procedures for Antennas, ANSI/IEEE Std.
149-1979, IEEE, New York; John Wiley Distributors.